

Nanoscopic friction as a probe of local phase transitions

Robert Szoszkiewicz and Elisa Riedo

Citation: *Appl. Phys. Lett.* **87**, 033105 (2005); doi: 10.1063/1.1995954

View online: <http://dx.doi.org/10.1063/1.1995954>

View Table of Contents: <http://apl.aip.org/resource/1/APPLAB/v87/i3>

Published by the [American Institute of Physics](#).

Additional information on *Appl. Phys. Lett.*


Journal Homepage: <http://apl.aip.org/>

Journal Information: http://apl.aip.org/about/about_the_journal

Top downloads: http://apl.aip.org/features/most_downloaded

Information for Authors: <http://apl.aip.org/authors>

ADVERTISEMENT



AIP | Applied Physics Letters

Accepting Submissions in
Biophysics and Bio-Inspired Systems

Submit Today

AIP
Publishing

Nanoscale friction as a probe of local phase transitions

Robert Szoszkiewicz and Elisa Riedo^{a)}

School of Physics, Georgia Institute of Technology, 837 State Street, Atlanta, Georgia 30332

(Received 11 February 2005; accepted 2 June 2005; published online 11 July 2005)

We study nanoscale friction forces between an atomic force microscope tip and a glass sample. We show how and why it is possible to tune friction forces in a predictable way by changing either the sample temperature, or the humidity in the experimental chamber. We relate the friction behavior to confined water phase transitions. We find that the water gas-liquid phase diagram is the same at the macroscopic scale as at the nanoscale tip-sample contact. © 2005 American Institute of Physics. [DOI: 10.1063/1.1995954]

The nanoscale behavior of adhesion and friction forces is arousing more and more interest in science and technology.^{1,2} In science, nanoscale studies of these forces permit to shed light on the atomic origin of several phenomena, such as nanoscale phase transitions³ and hydrophobic forces.⁴ In technology, there is an urgent demand for a better control of friction and adhesion forces in several nanoscale devices, for example, microelectro mechanical systems (MEMS), hard disks, and nanomotors.

It is well known that friction and adhesion forces are strongly dependent on the environmental humidity.^{5,6} This dependence is due to the formation of water menisci between the contacting surfaces. Each meniscus gives rise to what is called capillary force. The capillary force is an adhesive force due to a smaller pressure inside the liquid meniscus compared to the external gas pressure. This difference of pressure is inversely proportional to the effective radius of curvature of the meniscus. From classical thermodynamics consideration it is possible to establish a relationship between the radius of curvature of the meniscus (r_K), and (i) the temperature T , (ii) the vapor pressure P , and (iii) the saturated vapor pressure $P_s(T)$.^{7,8}

$$\frac{1}{r_K} = \frac{k_B T}{\gamma V_M} \ln\left(\frac{P}{P_s(T)}\right), \quad (1)$$

where V_M is the molecular volume of the liquid and γ is the liquid tension. We stress the fact that P_s depends on the temperature and it defines the pressure versus temperature borderline between the liquid and gas phase. For water in ambient atmosphere r_K is about 1 nm. This means that in nanoscale interstices water menisci form spontaneously, giving rise to high adhesive forces that can threaten the reliability of devices such as MEMS.

Recently, it has been demonstrated that it is possible to study the kinetics of capillary condensation at the nanoscale by means of velocity-dependent friction experiments with an atomic force microscope (AFM) nanosized tip.⁸⁻¹⁰ It remains unclear if the classical thermodynamics laws that regulate the capillary condensation at the macroscopic scale, such as the temperature dependence of P_s , are still valid at the nanoscale.

In this letter, we show how and why it is possible to obtain the same nanofriction versus velocity curves by changing either the sample temperature or the humidity in

the experimental chamber. We use these findings to study water capillary condensation at the nanoscale. We find that the temperature dependence of P_s is the same at the macroscopic scale as at the nanoscale tip-sample contact.

Friction forces (F_F) as a function of the sliding velocity v , have been investigated by means of an AFM (PicoPlus® from Molecular Imaging) operating in a controlled atmosphere. We use a hydrophilic silica glass substrate (from Fisher Scientific) with root mean square roughness of about 1 nm over 1 μm^2 areas. We use hydrophilic silicon AFM tip (from Nanosensors) with radius of 50 ± 10 nm as imaged by a scanning electron microscope after the measurements. Our rectangular cantilever has a normal spring constant of 0.1 N/m. We can vary the humidity in the experimental chamber ($\text{RH}_{\text{buffer}}$), from less than 0.05 up to 0.7, higher humidities have been avoided for the risk of electrical breakdown. In our AFM, a high-accuracy control system allows closed-loop control of the sample temperature (T_{sample}) with a precision of 0.1 °C. The temperature stage is designed for low vertical expansion or contraction and it works in air and in liquids from -10 to 100 °C.

Figure 1(a) shows friction versus velocity curves at different $\text{RH}_{\text{buffer}}$. The temperature of the experimental chamber (T_{buffer}) and T_{sample} are kept constant and equal to 20 °C. The evolution of these curves with $\text{RH}_{\text{buffer}}$ can be understood by considering that a water bridge can form only when there is enough time to overcome the formation energy barrier (low velocity), or when this energy barrier is enough low (high humidity).⁸ In Fig. 1(a) we can identify three different regimes. For very low humidities no water bridges can form at any velocity and the friction forces are very low (regime I). For very high humidities a quasistationary single water meniscus is formed between the tip and the sample at any velocity and the friction is high (regime III). For intermediate humidities we observe two plateaus at low (regime III) and high velocities (regime I), and in between the friction decreases with the velocity (regime II). This decreasing has been explained with a time-dependent formation of water bridges at the tip-sample contact.^{8,9}

The friction behavior shown in Fig. 1(a) can be reproduced by performing friction versus velocity curves at different T_{sample} , for a fixed buffer temperature and humidity [see Fig. 1(b)]. The similarity between Figs. 1(a) and 1(b) can be understood by doing two considerations. First, the friction versus velocity behavior depends on the relative humidity at the tip-surface contact. Thus, the same F_F versus v curves can be obtained either for a given humidity everywhere in

^{a)}Electronic mail: elisa.riedo@physics.gatech.edu

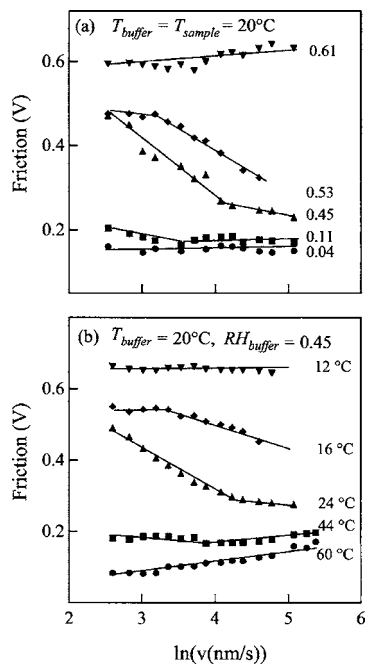


FIG. 1. Friction versus velocity: (a) for $T_{\text{buffer}}=T_{\text{sample}}=20^\circ\text{C}$ while varying $\text{RH}_{\text{buffer}}$ and (b) for $\text{RH}_{\text{buffer}}=0.45$ and $T_{\text{buffer}}=20^\circ\text{C}$ while varying T_{sample} .

the experimental chamber, or for the same humidity only at the tip-surface contact. Second, a change of the sample temperature is associated with a change of the local humidity at the glass surface.¹¹ More precisely, the definition of relative humidity is the following:

$$\text{RH} = P/P_S(T). \quad (2)$$

By fixing the relative humidity and temperature of the experimental chamber, we fix P everywhere in the experimental chamber, that is, also locally at the glass surface:¹²

$$P = \text{RH}_{\text{buffer}} P_S(T_{\text{buffer}}), \quad (3)$$

whereas by changing the sample temperature we change P_S locally. As a result, the curves in Fig. 1(b) at different T_{sample} for fixed $\text{RH}_{\text{buffer}}$ and T_{buffer} are equivalent to curves at different local relative humidity RH_{local} :

$$\text{RH}_{\text{local}} = P/P_S^{\text{local}}(T), \quad (4)$$

where P_S^{local} is the saturated pressure of water at the nanoscopic tip-sample contact.

To extract some quantitative information on the phase transitions at the nanoscale, we assume that the friction

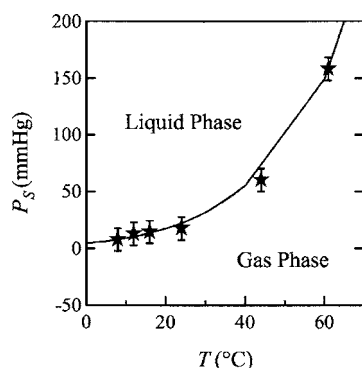


FIG. 2. Experimental values of $P_S^{\text{local}}(T)$ (scatter stars) compared with the macroscopic values of $P_S(T)$ (solid line).

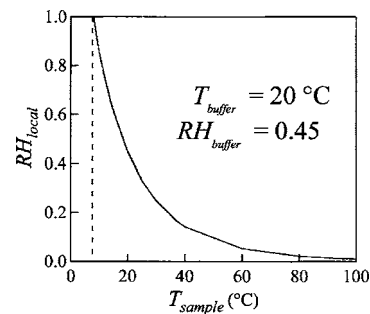


FIG. 3. RH_{local} as a function of T_{sample} calculated from Eqs. (3) and (4) by using the macroscopic values of $P_S(T)$.

curves in Figs. 1(a) and 1(b) are the same when RH_{local} in (b) is equal to $\text{RH}_{\text{buffer}}$ in (a). By comparing the Figs. 1(a) and 1(b) we find five values of $\text{RH}_{\text{local}}(T_{\text{sample}})$. These values are used to determine P_S at the nanoscale as a function of the temperature, by taking into account Eqs. (3) and (4):

$$P_S^{\text{local}}(T_{\text{sample}}) = \frac{\text{RH}_{\text{buffer}} P_S(T_{\text{buffer}})}{\text{RH}_{\text{local}}(T_{\text{sample}})}. \quad (5)$$

In Fig. 2 we show the phase diagram of water at the macroscopic scale (solid line)¹³ and the obtained local values of P_S . The experimental point $\text{RH}_{\text{local}}(T_{\text{sample}}=8^\circ\text{C})=1$ has been found by observing a sudden change of F_F versus v for $T_{\text{sample}} \leq 8^\circ\text{C}$. More precisely, for $T_{\text{sample}} \leq 8^\circ\text{C}$, F_F sharply increases with v for any velocity, indicating that a thick water layer has condensed on the surface (not shown here). This is confirmed by the experiments described in the next paragraph. Figure 3 shows RH_{local} as a function of T_{sample} obtained from Eq. (4) by using macroscopic values of $P_S(T)$. According to Fig. 3 the curves in Figs. 1(a) and 1(b) are the same when $\text{RH}_{\text{buffer}}$ in (a) is equal to RH_{local} in (b). This result together with the results reported in Fig. 2 lead to the conclusion that water gas-liquid phase diagram is the same at the macroscopic scale as well as at the nanoscopic tip-sample contact.

A strong indication that $P_S(T)$ follows the same behavior at the macro- and nanoscale is also given by normal force-distance curves. We have measured the normal force versus tip-sample distance while the tip approaches the glass surface at different T_{sample} for $\text{RH}_{\text{buffer}}=0.45$ and $T_{\text{buffer}}=20^\circ\text{C}$ (see Fig. 4). For $T_{\text{sample}} > 8^\circ\text{C}$, the distance at which the tip snaps into contact with the glass surface, the snap-in distance, is less than 5 nm, as expected for van der Waals forces and capillary forces in presence of few monolayers of water adsorbed on the glass surface. However, when $T_{\text{sample}} \leq 8^\circ\text{C}$

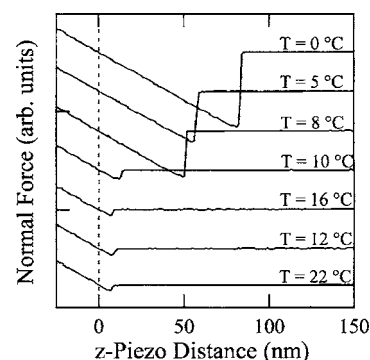


FIG. 4. Force versus distance curves taken at different T_{sample} .

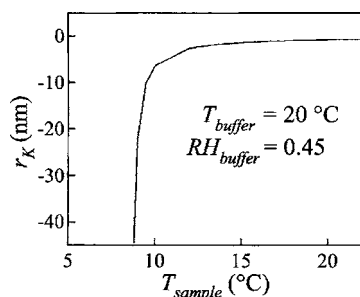


FIG. 5. r_K as a function of T_{sample} as resulting from Eq. (1) by using the macroscopic values of $P_S(T)$.

the snap-in distance becomes suddenly larger, about 50 nm. The snap-in distance has roughly three contributions coming from the van der Waals attraction, the capillary force and the water film present on the surfaces. The snap-in distance due to van der Waals forces is always smaller than few nanometers at all humidities. A sharp increase of the snap-in distance has thus to be related with an increase of the Kelvin radius and the water film thickness on the surfaces.⁷ The Kelvin equation (1) predicts a gas-liquid phase transition for $RH=1$; that is, r_K becomes infinite when $P=P_S(T)$. If we solve Eq. (5) with $RH_{\text{local}}=1$, $RH_{\text{buffer}}=0.45$, $T_{\text{buffer}}=20$ °C and macroscopic values of $P_S(T)$, we find $T_{\text{sample}}=8$ °C (see Fig. 5), in excellent agreement with the experiments.

In conclusion, we have shown how and why it is possible to tune friction forces in a controlled manner by changing either the sample temperature or the buffer humidity. These findings can help in the design of micro- or nanomotors. Furthermore, we have related nanofriction forces and force-distance curves to water capillary condensation. We conclude that the water gas-liquid phase diagram is the same at the macroscopic scale as well as at the nanoscopic tip-sample contact.

This work was supported by the National Science Foundation under Grant No. DMR-0405319 and by the Petroleum Foundation.

- ¹E. Riedo, E. Gnecco, R. Bennewitz, E. Meyer, and H. Brune, *Phys. Rev. Lett.* **91**, 084502 (2003).
- ²B. N. J. Persson, *Sliding Friction: Physical Principles and Applications*, in *NanoScience and Technology*, 2nd ed. (Springer, Berlin, 2000).
- ³Y. Zhu and S. Granick, *Phys. Rev. Lett.* **87**, 096104 (2001).
- ⁴J. Tyrrell and P. Attard, *Phys. Rev. Lett.* **87**, 176104 (2001).
- ⁵L. Sirghi, *Appl. Phys. Lett.* **82**, 3755 (2003).
- ⁶J. S. M. Scherge and X. Li, *Tribol. Lett.* **6**, 215 (1999).
- ⁷L. Fisher and J. Israelachvili, *J. Colloid Interface Sci.* **80**, 528 (1981).
- ⁸E. Riedo, I. Palaci, C. Boragno, and H. Brune, *J. Phys. Chem. B* **108**, 5324 (2004).
- ⁹E. Riedo, F. Levy, and H. Brune, *Phys. Rev. Lett.* **88**, 185505 (2002).
- ¹⁰L. Bocquet, E. Charlaix, S. Ciliberto, and J. Crassous, *Nature (London)* **396**, 735 (1998).
- ¹¹We assume that in our experiments temperature has no major effect besides modifying the relative humidity. This is confirmed by our unpublished results studying F_F versus $\ln v$ at $RH_{\text{buffer}}=4\%$ and $T_{\text{sample}}=20, 45,$ and 60 °C. At all three temperatures, F_F increases slightly with $\ln v$, in agreement with the curve at $RH_{\text{buffer}}=4\%$ in Fig. 1(a). However, F_F absolute values are lower at higher T ; thus F_F versus $\ln v$ curves appear shifted towards lower F_F values by increasing T . We underline that this shift is only 0.1 V as compared to F_F variations of about 0.5 V appearing in the measurements at $RH_{\text{buffer}}=45\%$ [see Fig. 1(b)]. We would like also to remark that the formation of capillary bridges is a thermally activated phenomenon. However, in this case the thermally activation would play a role only if we had changed T_{buffer} and not only T_{sample} . This topic is treated in detail in an upcoming publication.
- ¹²In our study, we assume that the pressure is uniform in the experimental chamber; that is, also close to the heated sample. This assumption is based on the fact that at standard conditions ($P=1$ atm, $T=298$ K) the mean time between collisions in air is about 150 ps. Since in our experiments we work in undersaturated conditions (maximum $T=60$ °C) and the time during which the AFM tip stays in contact with the surface is always longer than 1 ms, we conclude that during our measurements the pressure at the surface and the pressure in the buffer are at dynamic equilibrium and they have the same average value.
- ¹³*Handbook of Chemistry and Physics*, edited by D. R. Lide (CRC Press, Boca Raton, FL, 2002–2003).